Proceedings of Global Power and Propulsion Society
ISSN-Nr: 2504-4400
GPPS Xi'an21
18th – 20th October, 2021
www.gpps.global

GPPS-TC-2021-0252

Assessment of Finite Rate Chemistry Combustion Models in a Turbulent Dilute Ethanol Spray Flame

Yu Yin
School of Aerospace Engineering, Tsinghua University
yin-y16@mails.tsinghua.edu.cn
Beijing, China

Tianwei Yang
School of Aerospace Engineering, Tsinghua University
ytw16@mails.tsinghua.edu.cn
Beijing, China

Hua Zhou
Institute for Aero Engine, Tsinghua University
zhouhua@mail.tsinghua.edu.cn
Beijing, China

Zhuyin Ren
Institute for Aero Engine, Tsinghua University
zhuyinren@mail.tsinghua.edu.cn
Beijing, China

ABSTRACT

Spray combustion is of practical importance to various propulsion systems, though challenging for quantitative predictions that require proper modelling of flow and mixing, spray evaporation, interphase mass and energy coupling, as well as turbulence-chemistry interactions. In this study, simulations of a benchmark ethanol spray flames with partial pre-vaporization are performed with four combustion models at different levels of closure to provide a head-to-head comparative analysis on the closure effects of the crucial turbulence-chemistry interaction. The evaluation is carried out in the context of Reynolds-averaged Navier-Stokes simulations for the carrier-phase taking advantage of the simple jet configuration, together with a Lagrangian discrete phase model (DPM) for tracking the disperse spray droplets. The predictions are compared against experimental data including velocity, and temperature, clearly demonstrating the trend of improvement with increasing sophistication in TCI modelling from characteristic time scale model, laminar finite rate, eddy dissipation concept, and transported probability density function (TPDF). The TPDF model shows good agreement with the experimental data for temperature. Takeno flame index and the evolution of composition scattering in mixture fraction space suggest that the flame exhibits a mixed mode of combustion, i.e., nonpremixed dominant but with a significant level of premixedness in the fuel rich region.

INTRODUCTION

Spray combustion has a wide range of practical applications, including internal combustion engines, aviation gas turbines, and liquid-propellant rockets. Turbulent spray combustion involves multi-physical processes such as primary and secondary atomization, interparticle collisions, evaporation, mixing, and chemical reactions, occurring simultaneously and coupled in a strong manner. These fully coupled multi-physical processes with complex turbulence-chemistry interaction make predictive simulations of turbulent spray flames quite challenging. Dilute spray combustion is ideal for studying turbulence–chemistry interaction considering that the droplet concentration is low and the complicated atomization, collision and coalescence of droplets can be neglected.

For dilute spray flames, the Eulerian-Lagrangian simulation approach is in general adopted, in which the continuous gaseous phase is resolved by solving the Navier-Stokes equations, while the dispersed liqiud phase is solved by Lagrangian tracking droplets. Over the past decade, significant progress has been made on the development of physiochemical models and computational methods for improving the simulation accuracy of turbulent dilute spray flames. Chrigui (Chrigui et al, 2012; Chrigui et al, 2013) performed simulations of acetone spray flame and ethanol spray flame using flamelet generated manifold (FGM) with presumed PDF method. Rittler (Rittler et al, 2015) validated the premixed flamelet generated manifold approach (PFGM) combining a presumed PDF method, tabulated chemistry and artificial thickening for the ethanol flame. Honhar (Honhar et al, 2017) and Heye (Heye et al, 2013) performed RANS and LES calculations of an ethanol spray flame using the transported PDF method to resolve turbulence-chemistry interactions Hu (Hu et al, 2017) performed simulations of an ethanol spray flame using a spray flamelet approach combined with transported PDF method for solving mixture fraction. Sacomano Filho (Sacomano Filho et al, 2020) investigated the turbulence-flame interactions in an ethanol spray flame with dynamic flame surface wrinkling in the context of the artificially thickened flame approach.

High-fidelity simulation of turbulent spray flames strongly depends on accurate combustion models. In general, the models for gaseous phase have been extended to simulate the dilute spray combustion, and they can be classified into two main categories, i.e. the finite rate chemistry models and the flamelet models. Examples of finite rate chemistry models are the laminar finite rate (LFR) model, the perfectly-stirred reactor (PSR) model (Lysenko et al, 2014), the Eddy Dissipation Concept (EDC) model (Gran & Magnussen, 1996), the thickened flame model (TFM) (Colin et al, 2000), and the transported probability density function (TPDF) model (Pope, 1985). Examples of flamelet models are the laminar flamelet model (Peters, 1984), the flamelet/progress variable (FPV) model (Pierce & Moin, 2004), and the Lagrangian flamelet model (Pitsch & Steiner, 2000). Finite rate chemistry models are attractive for turbulent spray simulation as they are applicable to different combustion modes without the assumption of specific flame configuration and flamelet.

Regardless of many successful investigations of spray flame using finite rate combustion, most of them employing simplified chemical kinetics (Emami et al, 2019; Menon & Patel, 2006; Pei et al, 2013). There have been some comparative studies of combustion models for gaseous flames (Fedina et al, 2017; Panchal et al, 2019; Yang et al, 2020) but few in spray combustion (Piehl et al, 2018; Wang et al, 2019). The purpose of this work is to evaluate the capability of finite rate chemistry models and to investigate the effects of turbulence-chemistry interaction closure on the prediction of spray flames' structure. To this end, four different finite rate chemistry models at different closure levels of turbulence-chemistry interaction, namely the characteristic timescale (CTS) model, the LFR model, the EDC model and TPDF model are employed to simulate the spray flames with detailed chemistry, in order to provide a head-to-head comparative analysis on the effects of the crucial turbulence-chemistry interaction closure.

METHODOLOGY

The finite-rate chemistry effects in the turbulent dilute ethanol spray flame EtF2 of the Sydney Spray Burner (Gounder et al, 2012) are assessed in two-way coupled two-phase simulations in which the continuous gaseous phase is resolved by solving the governing equations for fluid flows and compositions fields (i.e., species and energy) if applicable with a low-Mach number solver, while the dispersed liqiud phase is solved by tracking the spray droplets in a Lagrangian frame. Considering the basic jet configuration in spray flame EtF2, the Reynolds-averaged Navier–Stokes (RANS) equations are solved with emphasis on analyzing turbulence-chemistry interaction closure for composition fields. The dispersion of liquid droplets due to turbulence is simulated using a discrete random walk model. For two-way spray–flow interactions, the spray droplets exchange mass, momentum, and energy with the surrounding gaseous phase through the under-relaxed spray source terms.

Turbulent dilute ethanol spray flame EtF2

The burner consists of three concentrically arranged streams: a jet, a pilot and a primary coflow. Liquid fuel is atomized by an ultrasonic nebulizer located 215 mm upstream of the jet exit plane and the generated droplets are then transported downstream in a central tube with a diameter of D=10.5 mm, where some evaporation has occurred upstream of the nozzle exit. An annular pilot composed of combustion products from a stoichiometric acetylene/hydrogen/air mixture is used to stabilize the spray flame with an outer diameter of 25 mm. The velocity of the burnt pilot gas is 11.6 m/s and the adiabatic pilot temperature is 2493 K, according to the bulk velocity of the unburnt gas maintained at 1.5 m/s. The burner is installed vertically in a wind tunnel providing an air coflow of 4.5 m/s. The diameter of coflow surrounding the burner is 104 mm. Figure 1 shows the simulation domain and the inflow configuration. The inflow conditions of EtF2 are given in Table 1. The detailed description of experimental device is given by Ref. (Gounder et al, 2012).

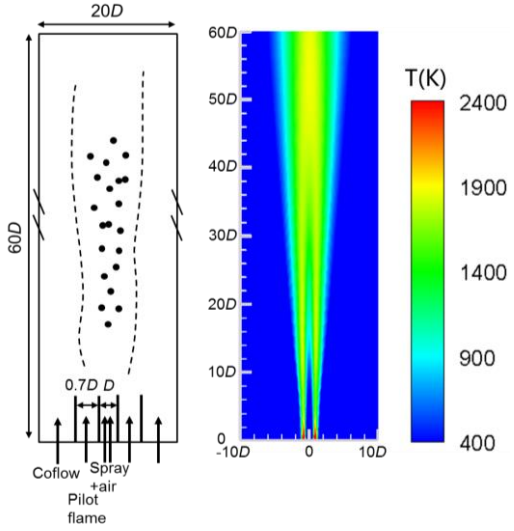

Figure 1 Schematic of the spray flame configuration. The jet diameter D is 10.5 mm.

Table 1 Inlet conditions of the ethanol spray flames EtF2

Ethanol combustion	EtF2
Bulk jet velocity (m/s)	36
Carrier mass flow rate (g/min)	225
Liquid fuel rate at jet exit (g/min)	66.3
Vapor fuel rate at jet exit (g/min)	8.7
Jet Reynolds number	30500

Finite-rate chemistry combustion models

Four combustion models at different levels of closure ranging from the characteristic time scale model to the most sophisticated transported PDF are analyzed. The transport equations for the mean mass fractions of species in spray combustion are given by

$$\frac{\partial \bar{\rho}\widetilde{Y_i}}{\partial t}+\frac{\partial}{\partial x_j}\left(\bar{\rho}\widetilde{u_j}\widetilde{Y_i}\right)=\frac{\partial}{\partial x_j}\left(\bar{\rho}\bar{D_i}\frac{\partial \widetilde{Y_i}}{\partial x_j}\right)-\frac{\partial q_{j,Y_i}}{\partial x_j}+\bar{\dot{\omega}}_i+\overline{S_{Y_i}}, \tag{1}$$

where $\bar{\rho}$ is the averaged density, $\widetilde{Y_i}$ is the averaged mass fraction of ith species, D_i is the molecular diffusivity, $\bar{\dot{\omega}}_i$ is the mean chemical source term and $\overline{S_{Y_i}}$ is the averaged source term due to mass exchange between dispersed phase and the continuous phase. The unresolved scalar flux, $q_{j,Y_k}=\bar{\rho}\widetilde{u_jY_i}-\bar{\rho}\widetilde{u_j}\widetilde{Y_i}$, are described using a gradient assumption as $q_{j,Y_i}=-\frac{\mu_t}{\rho Sc_t}\frac{\partial \widetilde{Y_i}}{\partial x_j}$. The mean chemical source term $\bar{\dot{\omega}}_k$ is closed using the combustion model together with a chemical mechanism. In this study, a detailed mechanism consisting of 50 species and 235 elementary reactions is employed for ethanol oxidation (2011). The characteristic timescale (CTS) model assumes that for each computational cell, species mass fractions relax to the local chemical equilibrium state over a characteristic time determined by flow time scale and chemical time scale. The CTS model is applicable to a wide range of turbulent reaction flows though may not be accurate due to the simple treatment of chemical kinetics. For computational efficiency, the local chemical equilibrium composition is tabulated and reused on the fly with the in situ adaptive tabulation. For laminar finite rate model, it relies on a direct computation of the mean chemical source term with the cell mean composition by neglecting effect of cell composition fluctuation. For eddy dissipation concept model, it assumes that the reaction takes place in small turbulent structures (called fine scales), which have the same sizes as the Kolmogorov microscale. According to (Gran & Magnussen, 1996), assuming that the reactants are uniformly mixed in these fine structures, the cell mean reaction rate is determined by the rate of mass transfer of ith species from the fine structure to the surrounding cell fluid, i.e.,

$$\overline{\dot{\omega}_i}=\bar{\rho}\frac{\xi^{*2}}{\tau^*}\left(Y_i^{\mathbf{0}}-Y_i^*\right), \tag{2}$$

where ξ^* is the length fraction of cell occupied by fine structure, and τ^* is the time scale for the mass transfer between the fine structure and the surrounding fluid. The superscripts * and 0 denote fine structure and surrounding cell fluid quantities, respectively. The EDC implemented in ANSYS Fluent is employed for comparison, although recent enhancements for EDC have been reported such as the one for MILD combustion (Lewandowski et al, 2020). As an alternative to solve the species and energy equations, a transport equation is derived for their one-point one-time joint probability density function (PDF). The PDF can be intepreated as the probability of the fluid being at individual composition state. The one-point one-time PDF is denoted by $P(\boldsymbol{\psi},\eta;x,t)$, where $\{\boldsymbol{\psi},\eta\}$ are the sample space variables of the corresponding thermochemical composition vector $\boldsymbol{\phi}=(Y_1,Y_2,\dots,Y_{N_s},h)$. The transport equation of PDF can be written as

$$\begin{aligned}\frac{\partial P}{\partial t}+\frac{\partial(\widetilde{u_i}P)}{\partial x_i}-\frac{\partial}{\partial x_i}\left(\bar{\rho}D_t\frac{\partial P/\bar{\rho}}{\partial x_i}\right)=&-\sum_{\alpha=1}^{n_s}\frac{\partial}{\partial \psi_\alpha}\left[-\left\langle\frac{\partial J_i^\alpha}{\partial x_i}\middle|\boldsymbol{\psi},\eta\right\rangle+\omega_\alpha(\boldsymbol{\psi},\eta)+\left(Y_\alpha^f-\psi_\alpha\right)S_c^m\right]P\\&-\frac{\partial}{\partial \eta}\left[-\left\langle\frac{\partial J_i^h}{\partial x_i}\middle|\boldsymbol{\psi},\eta\right\rangle+\omega_h(\boldsymbol{\psi},\eta)+\left(S_c^h-\eta S_c^m\right)\right]P+S_c^mP,\end{aligned} \tag{3}$$

where J_i^α is the molecular diffusion flux, J_i^h is the specific enthalpy flux vector due to molecular transport, Y_α^f is the mass fraction of αth species in the droplet vapor, and D_t is the turbulent diffusivity. ω_α and ω_h are the source terms due to chemical reactions. $S_c^m=\widehat{S^m|\boldsymbol{\psi},\eta}$ is the conditional evaporation rate, and $S_c^h=\widehat{S^h|\boldsymbol{\psi},\eta}$ is the conditional energy source term. In the TPDF method, the chemical source term is closed naturally and no additional modelling is required. The conditional mixing/diffusion term needs to be treated by micro-mixing models. In the present work, the Euclidean minimum spanning tree (EMST) model (Subramaniam & Pope, 1998) is used.

Simulation Settings

Table 2 shows the numerical settings. An incompressible, pressure-based, steady solver was coupled with the standard $k-\varepsilon$ turbulence model. The CFD commercial code ANSYS Fluent was used to solve the conservation equations of mass, momentum, species, energy and turbulence quantities.

Table 2 Numerical settings

Domain	3D
Solver	Steady, pressure based
Turbulence model	Standard $k-\varepsilon$ model with C_μ=0.09, $C_{\varepsilon 1}$=1.6, $C_{\varepsilon 2}$=1.92, σ_k=1.0, σ_ε=1.3, energy Prandtl number 0.85, turbulent Schmidt number 0.7
ISAT error tolerance	10^{-4}
Discretization	Second order for pressure, coupled scheme for pressure–velocity coupling, second order upwind for momentum, species and k
Material	Incompressible ideal gas, mixing law for C_p, ideal gas mixing law for thermal conductivity and viscosity, kinetic theory for mass diffusivities

For the dispersed phase description, a standard discrete phase approach (Dukowicz, 1980) has been adopted. Parcels of droplets were injected into the simulation domain with specified diameter and velocity. The droplets were subject to drag force and were assumed to be spherical with a convection-diffusion vaporization model, while the Ranz–Marshall approach (Ranz & Marshall, 1952) was used for heat transfer. The stochastic approach known as discrete random walk model (Gosman & Ioannides, 1983), was employed to account for turbulent dispersion.

The cylindrical simulation domain consists of 1.3 million hexahedral cells, which is 10 jet diameters in radial direction and 60 diameters in axial direction. The local refinement of mesh is employed to resolve the near field and the jet centerline with a minimum size of 0.2 mm. Convergence tests using a finer grid (1.5x) have been performed to make sure that simulation has reached numerical convergence given the current grid resolution.

The radial distribution of the gas-phase averaged velocity measured near the nozzle exit plane (x/D = 0.3) is used as the boundary condition of the gas-phase velocity. The inlet turbulence intensity of the carrier phase is set to 5%. The pilot and wind tunnel inflows are approximated to be laminar. The total number of 15000 particle parcels are injected into the simulation domain at the nozzle exit plane (x/D = 0). The initial droplet size is specified by the Rosin-Rammler distribution, and the diameter distribution is consistent with the diameter distribution data of the most upstream collection positon (x/D = 0.3).

Figure 2 shows comparison of the mean axial gas-phase velocity at x/D = 0.3, 10, 20 and 30. The mean axial velocity profiles are generally well captured compared with the experiments at different axial locations for different combustion models, indicating the flow field is well resolved with utilized boundary conditions under the standard $k-\varepsilon$ model.

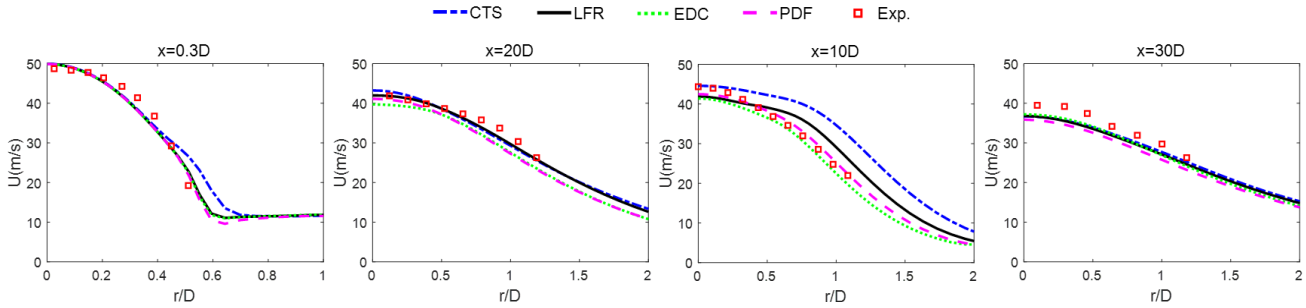

Figure 2 Radial profiles of mean axial component of the gas velocity (*U*) at different axial locations x/D for four combustion models.

RESULTS AND DISCUSSION

Radial profiles of gaseous and discrete phases

Measured and calculated radial profiles of the gas-phase mean temperature at different axial locations are shown in Figure 3. It is obviously that the results obtained from the PDF model yields better agreement with the experimental measurements at all axial locations compared to other models. The spatial location of peak temperature, as an indication of the mean reaction zone, is well predicted for these four combustion models, with a little wider flame brush than in the experiments. Over-predictions of peak temperature are observed for the CTS, LFR, and EDC models, where the maximum deviations are estimated to be about 38% for CTS model, about 32% for LFR model and about 23% for EDC model at r/D = 30. The peak temperature is reasonably well predicted for PDF model at r/D = 10, with slight over-predictions at r/D = 20 (of order 8%) and at r/D = 30 (of order 7%).

For the dispersed phase, Figure 4 presents radial profiles of the mean axial and radial components of droplets velocities as well as the droplet SMD (Sauter mean diameter) at x/D = 10, 20, and 30, respectively. One can observe that the computed

mean axial velocity profiles agree reasonably well with experimental measurements for all the four models, though the CTS model predicts a little higher value at x/D = 10. Profiles of mean radial velocities, from four combustion models qualitatively follow a similar trend as in the experimental measurements. The predicted droplet SMD shows under-prediction compared to the experimental measurements with better agreement close to the centerline, and the deviation is larger at downstream. The under-prediction of the droplet SMD indicates that the predicted evaporation rate is higher, this is consistent with the slightly overpredicted temperature shown in Figure 3.

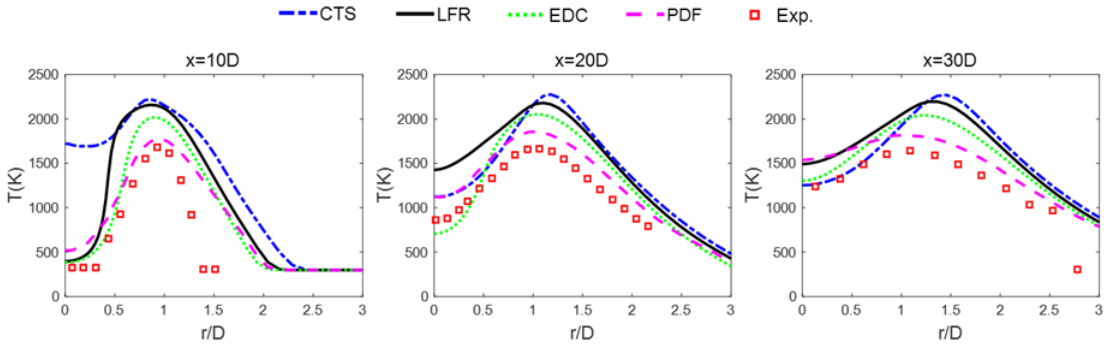

Figure 3 Radial profiles of gas-phase mean temperature (T) at different axial locations x/D for four combustion models.

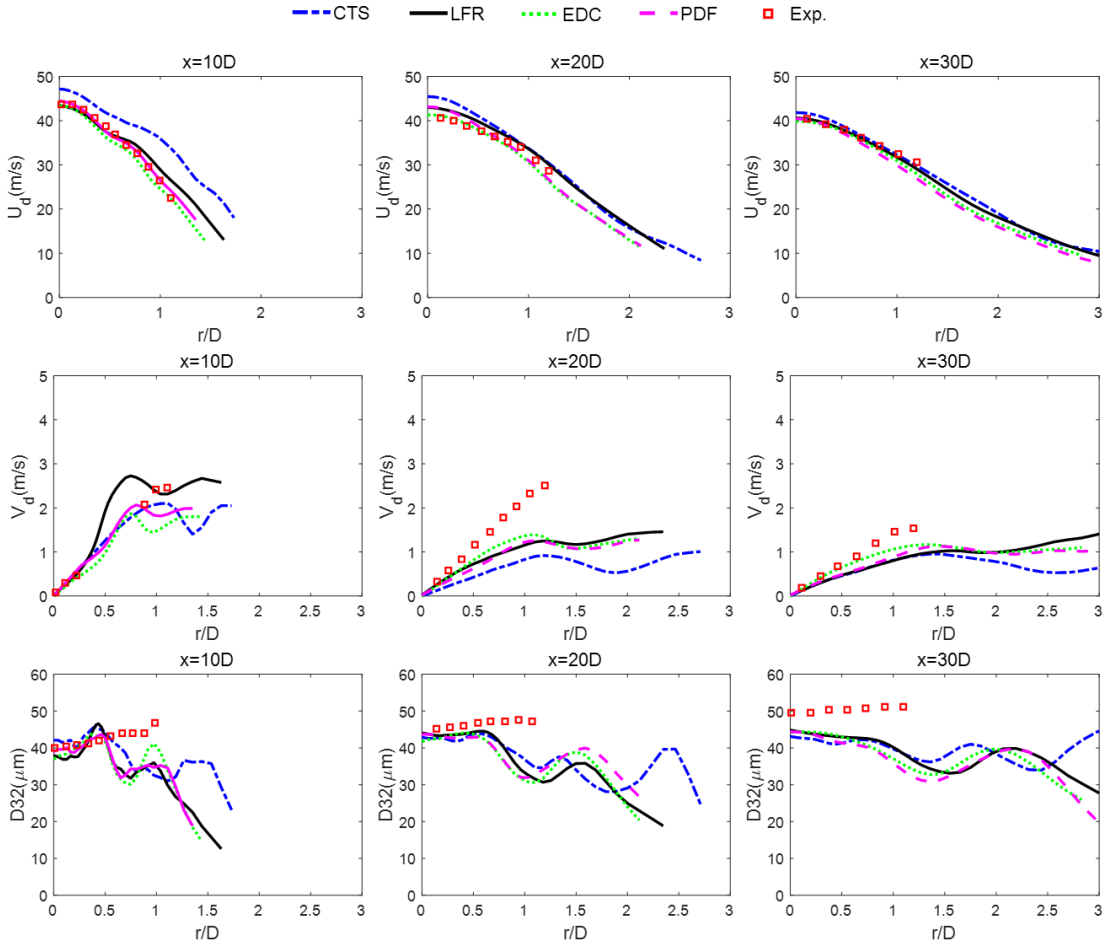

Figure 4 Radial profiles of the mean axial (U_d) and radial (V_d) components of droplets velocity as well as the Sauter mean diameter (D_{32}) at different axial locations x/D from four combustion models.

Flame structure analysis

Figure 5 shows the predictions of gas-phase Favre mean temperature and mixture fraction in the cross section along the centerline. As indicated by the mean temperature, the PDF model predicts a thicker flame with a lower flame temperature than others since the PDF model better accounts for scalar fluctuations. The maximum mixture fraction occurs on the centerline at around 300 mm downstream the nozzle as a combined effect of high droplet concentration and

evaporation rate. The maximum value of the mean mixture fraction is about 0.26 for CTS model, 0.23 for LFR model, and 0.22 for EDC and PDF model. The difference in mixture fraction indicates a different evaporation rate for each combustion model.

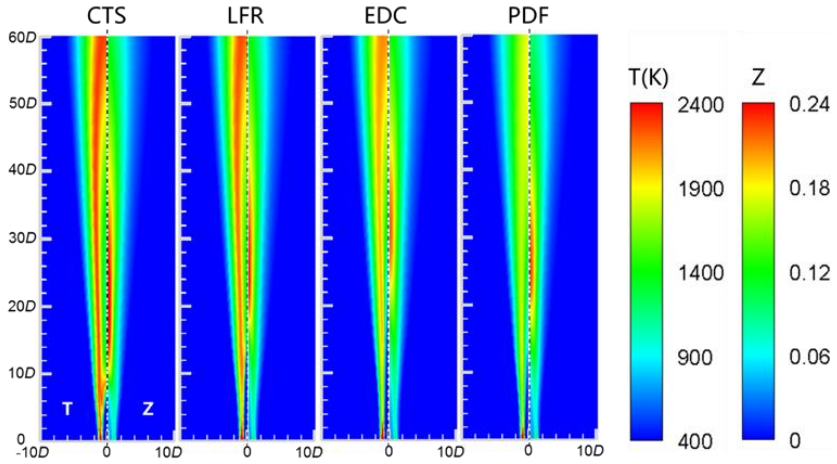

Figure 5 Contour plots of gas-phase Favre mean temperature (T) and mixture fraction (Z).

Mixed mode combustion occurs in spray flames, depending on the combined effects of evaporation and mixing, a spray flame could be either non-premixed or premixed dominated. The Takeno Flame Index (TFI), (Yamashita et al, 1996), shown in Figure 6, is a metric for the alignment between the gradient of the C_2H_5OH and O_2 mass fractions used to describe the mixing mode between the C_2H_5OH and O_2 such that $G = \nabla Y_{C2H5OH} \cdot \nabla Y_{O2}$. In the investigation of partially premixed gaseous and spray flames, Domingo et al. (Domingo et al, 2005) normalized G such that $\xi = G/|G|$ so $\xi > 0$ in premixed reaction zones and $\xi < 0$ in non-premixed reaction zones. This means that in premixed reaction zones (with $\xi > 0$) C_2H_5OH and O_2 are consumed in the same physical direction, while in non-premixed reaction zones (with $\xi < 0$) C_2H_5OH and O_2 are consumed in opposite directions. Evident from Figure 6, premixed regions most frequently occur near the nozzle-exit and in the inner part of the flame zone where droplets pre-evaporate and mix with air, while non-premixed regions most frequently occur in the part of the flame and the outer part of the flame zone. Hence, the fame EtF2 burns predominantly in a non-premixed mode. Compared to the PDF model, the EDC model predicts a large portion of premixed type of combustion. This is consistent with the findings from Figure 5, where the maximum mixture fraction predicted by the EDC model occurs at further downstream compared to the PDF model, resulting in a higher level of premixedness.

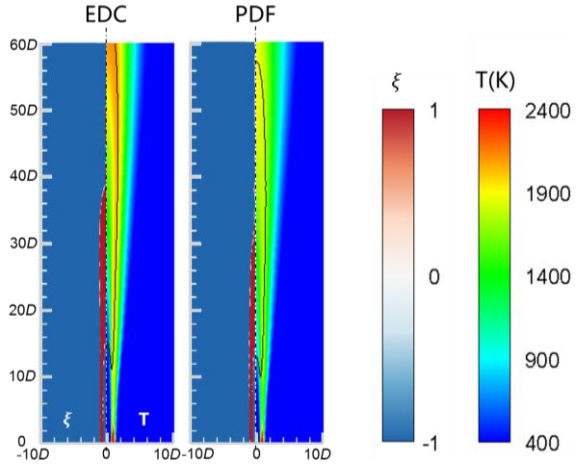

Figure 6 Identification of premixed (red) and diffusion (blue) flame zones by means of the Takeno flame index and gas-phase Favre mean temperature with isoline on $Z = 0.1004$.

Composition evolution in mixture fraction space

In this section, scatter plots of temperature in mixture fraction space are compared at different axial positions to investigate the local evolution of the flow and reaction fields. Figure7 shows scatter plots for temperature versus mixture fraction for axial bands of 0 < x/D < 10, 10 < x/D < 20, 20 < x/D < 30, 30 < x/D < 40, and 40 < x/D < 50. It is interesting to found that different flame patterns occur at different axial locations. For 0 < x/D < 10, the black dots clearly show a structure consisting of two branches. These are essentially two mixing lines, one represents the mixing between the pilot stream (Z = 0.09) and the coflow stream (Z = 0), the other represents the mixing between the central jet (Z = 0.037 to

account for pre-evaporated fuel) and the pilot stream. For 10 < x/D < 20 represented by blue dots, the two-branch structure persists when LFR, EDC or PDF model is employed. It is interesting to note that the branch on the right exhibits a broad change in temperature at a given certain mixture fraction. This is similar to the premixed flame with constant equivalence, illustrating a premixed type of combustion.This is because evaporation occurs at some distance from the flame front, allowing for adequate mixing between fuel and oxidizer, thus, leading to a premixed, variable equivalence ratio mixture that approaches the flame front. However, when CTS model is employed, the 'premixed branch' disappears as a result of the higher temperature and higher evaporation rate predicted by this model. At further downstream, i.e., x/D > 30, as most of the droplets get evaporated, the structures predicted by all four combustion models are close to the typical non-premixed flame, indicating a non-premixed dominated type of combustion.

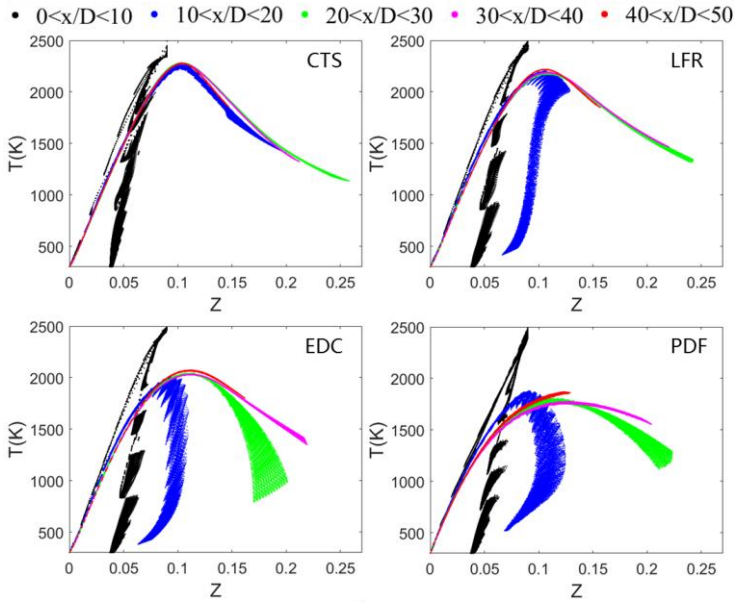

Figure 7 Scatter plots of the gas-phase mean temperature (*T*) against the mean mixture fraction (*Z*) inside axial bands 0<x/D < 10, 10 < x/D < 20, 20 < x/D < 30, 30 < x/D < 40, and 40 < x/D < 50 for four combustion models.

CONCLUSIONS

Simulations for Sydney ethanol flames ETF2 are performed using RANS approach with four finite-rate combustion models, including the CTS, LFR, EDC, and TPDF models. The liquid phase is modelled using a Lagrangian stochastic particle method together with models for the convective-diffusion droplet heating and evaporation. Two way coupling is adopted between the Eulerian flow field and the Lagrangian tracked particles.

The performance of four different finite-rate combustion models is studied for the different levels of closure of mean chemical reaction source term by comparing with experimental measurement. The mean droplet velocities are reasonably well predicted, while prediction of the fluctuating droplet velocity is less satisfactory, implying the deficiency of the random walk model for turbulent dispersion. The mean temperature is notably overpredicted by the CTS and LFR model, the EDC model shows some improvement for the prediction of the mean temperature on centerline but still overpredicts the peak temperature. In general, the TPDF model shows a better match with temperature measurements than other models. The combustion modes have been identified with Takeno flame index, and it is observed that the flame exhibits a mixed mode of combustion, i.e., nonpremixed dominant but with a significant level of premixedness in the fuel rich region. The statistics in mixture fraction space demonstrated the presence of a stratified premixed zone in the upstream and a typical non-premixed flame structure in the downstream.

ACKNOWLEDGMENTS

The work is supported by National Natural Science Foundation of China 91841302 and 52025062. Simulations are done with the computational resources from the Tsinghua National Laboratory for Information Science and Technology.

REFERENCES

Chemical-kinetic mechanisms for combustion applications, (2011). The San Diego Mechanism. Available online: http://combustion.ucsd.edu/.

Chrigui, M., Gounder, J., Sadiki, A., Masri, A. R. and Janicka, J. (2012). Partially Premixed Reacting Acetone Spray Using LES and Fgm Tabulated Chemistry. *Combustion and Flame*, 159(8), 2718-2741.

Chrigui, M., Masri, A. R., Sadiki, A. and Janicka, J. (2013). Large Eddy Simulation of a Polydisperse Ethanol Spray Flame. *Flow Turbulence and Combustion*, 90(4), 813-832.
Colin, O., Ducros, F., Veynante, D. and Poinsot, T. (2000). A Thickened Flame Model for Large Eddy Simulations of Turbulent Premixed Combustion. *Physics of Fluids*, 12(7), 1843-1863.
Domingo, P., Vervisch, L. and Reveillon, J. (2005). Dns Analysis of Partially Premixed Combustion in Spray and Gaseous Turbulent Flame-Bases Stabilized in Hot Air. *Combustion and Flame*, 140(3), 172-195.
Dukowicz, J. K. (1980). A Particle-Fluid Numerical-Model for Liquid Sprays. *Journal of Computational Physics*, 35(2), 229-253.
Emami, S., Jafari, H. and Mahmoudi, Y. (2019). Effects of Combustion Model and Chemical Kinetics in Numerical Modeling of Hydrogen-Fueled Dual-Stage Hvof System. *Journal of Thermal Spray Technology*, 28(3), 333-345.
Fedina, E., Fureby, C., Bulat, G. and Meier, W. (2017). Assessment of Finite Rate Chemistry Large Eddy Simulation Combustion Models. *Flow Turbulence and Combustion*, 99(2), 385-409.
Gosman, A. D. and Ioannides, E. (1983). Aspects of Computer-Simulation of Liquid-Fueled Combustors. *Journal of Energy*, 7(6), 482-490.
Gounder, J. D., Kourmatzis, A. and Masri, A. R. (2012). Turbulent Piloted Dilute Spray Flames: Flow Fields and Droplet Dynamics. *Combustion and Flame*, 159(11), 3372-3397.
Gran, I. R. and Magnussen, B. F. (1996). A Numerical Study of a Bluff-Body Stabilized Diffusion Flame .2. Influence of Combustion Modeling and Finite-Rate Chemistry. *Combustion Science and Technology*, 119(1-6), 191-217.
Heye, C., Raman, V. and Masri, A. R. (2013). LES/Probability Density Function Approach for the Simulation of an Ethanol Spray Flame. *Proceedings of the Combustion Institute*, 34, 1633-1641.
Honhar, P., Hu, Y. and Gutheil, E. (2017). Analysis of Mixing Models for Use in Simulations of Turbulent Spray Combustion. *Flow Turbulence and Combustion*, 99(2), 511-530.
Hu, Y., Olguin, H. and Gutheil, E. (2017). A Spray Flamelet/Progress Variable Approach Combined with a Transported Joint Pdf Model for Turbulent Spray Flames. *Combustion Theory and Modelling*, 21(3), 575-602.
Lewandowski, M. T., Parente, A. and Pozorski, J. (2020). Generalised Eddy Dissipation Concept for Mild Combustion Regime at Low Local Reynolds and Damk öhler Numbers. Part 1: Model Framework Development. *FUEL*, 278, 117743.
Lysenko, D. A., Ertesvag, I. S. and Rian, K. E. (2014). Numerical Simulations of the Sandia Flame D Using the Eddy Dissipation Concept. *Flow Turbulence and Combustion*, 93(4), 665-687.
Menon, S. and Patel, N. (2006). Subgrid Modeling for Simulation of Spray Combustion in Large-Scale Combustors. *AIAA Journal*, 44(4), 709-723.
Panchal, A., Ranjan, R. and Menon, S. (2019). A Comparison of Finite-Rate Kinetics and Flamelet-Generated Manifold Using a Multiscale Modeling Framework for Turbulent Premixed Combustion. *Combustion Science and Technology*, 191(5-6), 921-955.
Pei, Y., Hawkes, E. R. and Kook, S. (2013). A Comprehensive Study of Effects of Mixing and Chemical Kinetic Models on Predictions of N-Heptane Jet Ignitions with the Pdf Method. *Flow Turbulence and Combustion*, 91(2), 249-280.
Peters, N. (1984). Laminar Diffusion Flamelet Models in Non-Premixed Turbulent Combustion. *Progress in Energy and Combustion Science*, 10(3), 319-339.
Piehl, J. A., Samimi Abianeh, O., Goyal, A. and Bravo, L. (2018). Turbulent Spray Combustion Modeling Using Various Kinetic Solvers and Turbulence Models. *J. Eng. Gas Turbines Power*, 140(12).
Pierce, C. D. and Moin, P. (2004). Progress-Variable Approach for Large-Eddy Simulation of Non-Premixed Turbulent Combustion. *Journal of Fluid Mechanics*, 504, 73-97.
Pitsch, H. and Steiner, H. (2000). Large-Eddy Simulation of a Turbulent Piloted Methane/Air Diffusion Flame (Sandia Flame D). *Physics of Fluids*, 12(10), 2541-2554.
Pope, S. B. (1985). Pdf Methods for Turbulent Reactive Flows. *Progress in Energy and Combustion Science*, 11(2), 119-192.
Ranz, W. E. and Marshall, W. R. (1952). Evaporation from Drops .1. *Chemical Engineering Progress*, 48(3), 141-146.
Rittler, A., Proch, F. and Kempf, A. M. (2015). LES of the Sydney Piloted Spray Flame Series with the Pfgm/Atf Approach and Different Sub-Filter Models. *Combustion and Flame*, 162(4), 1575-1598.
Sacomano Filho, F. L., Hosseinzadeh, A., Sadiki, A. and Janicka, J. (2020). On the Interaction between Turbulence and Ethanol Spray Combustion Using a Dynamic Wrinkling Model Coupled with Tabulated Chemistry. *Combustion and Flame*, 215, 203-220.
Subramaniam, S. and Pope, S. B. (1998). A Mixing Model for Turbulent Reactive Flows Based on Euclidean Minimum Spanning Trees. *Combustion and Flame*, 115(4), 487-514.
Wang, Q., Jaravel, T. and Ihme, M. (2019). Assessment of Spray Combustion Models in Large-Eddy Simulations of a Polydispersed Acetone Spray Flame. *Proceedings of the Combustion Institute*, 37(3), 3335-3344.
Yamashita, H., Shimada, M. and Takeno, T. (1996). A Numerical Study on Flame Stability at the Transition Point of Jet Diffusion Flames. *Symposium (International) on Combustion*, 26(1), 27-34.
Yang, T., Xie, Q., Zhou, H. and Ren, Z. (2020). On the Modeling of Scalar Mixing Timescale in Filtered Density Function Simulation of Turbulent Premixed Flames. *Physics of Fluids*, 32(11).